tvst

Article

Tissue Responses and Wound Healing following Laser Scleral Microporation for Presbyopia Therapy

Yu-Chi Liu[1–3], Brad Hall[4], Nyein Chan Lwin[1], Ericia Pei Wen Teo[1], Gary Hin Fai Yam[1,3], AnnMarie Hipsley[4], and Jodhbir S. Mehta[1–3]

[1] Tissue Engineering and Stem Cell Group, Singapore Eye Research Institute, Singapore
[2] Singapore National Eye Centre, Singapore
[3] Duke-NUS Medical School, Singapore
[4] Ace Vision Group, Inc., Newark, CA, USA

Correspondence: Jodhbir S. Mehta, Singapore National Eye Centre, 11 Third Hospital Avenue, Singapore 168751. e-mail: jodmehta@gmail.com

Received: June 6, 2019
Accepted: December 27, 2019
Published: March 9, 2020

Keywords: presbyopia; laser; scleral wound healing

Citation: Liu Y-C, Hall B, Lwin NC, Teo EPW, Yam GHF, Hipsley A, Mehta JS. Tissue responses and wound healing following laser scleral microporation for presbyopia therapy. Trans Vis Sci Tech. 2020;9(4):6, https://doi.org/10.1167/tvst.9.4.6

Purpose: To investigate the postoperative inflammatory and wound-healing responses after laser scleral microporation for presbyopia.

Methods: Thirty porcine eyes were used for the optimization of laser intensities first. Six monkeys (12 eyes) received scleral microporation with an erbium yttrium aluminum garnet (Er:YAG) laser, and half of the eyes received concurrent subconjunctival collagen gel to modulate wound-healing response. The intraocular pressure (IOP) and the laser ablation depth were evaluated. The animals were euthanized at 1, 6, and 9 months postoperatively. The limbal areas and scleras were harvested for histologic analysis and immunofluorescence of markers for inflammation (CD11b and CD45), wound healing (CD90, tenascin-C, fibronectin, and HSP47), wound contraction (α–smooth muscle actin [α-SMA]), vascular response (CD31), nerve injury (GAP43), and limbal stem cells (P63 and telomerase).

Results: In the nonhuman primate study, there was a significant reduction in IOP after the procedure. Overall, the ablation depth was 76.6% to 81.2% at 1 month and slightly decreased to 71.5% to 72.7% at 9 months. Coagulative necrosis around the microporesores, as well as expression of CD11b, CD45, tenascin, fibronectin, HSP47, and GAP43, was distinct at 1 month but subsided with time. Collagen gel treatment significantly suppressed the upregulation of CD11b, CD45, fibronectin, and tenascin-C. The expression of CD90, α-SMA, and CD31 was minimal in all eyes.

Conclusions: The study demonstrated the course of inflammatory and wound-healing responses following laser scleral microporation. The tissue responses were small and self-limited, resolved with time, and were suppressed by concurrent collagen treatment. It provides a useful understanding of this new procedure.

Translational Relevance: The results would be helpful in the laser parameter modification to improve the long-term treatment stability.

Introduction

Presbyopia affects individuals older than 40 years and is the most common refractive error.[1] It currently affects approximately 2 billion people worldwide.[2] Presbyopia has been traditionally described by the "Helmholtz hypothesis," wherein the loss of elasticity of the lens with age results in a reduction in accommodation, causing presbyopia.[3] Brown[4] and Koretz et al.[5] further elucidated that presbyopia results from an age-related increase in lens thickness, decreasing the radius of curvature and the lens paradox. More recent studies have also demonstrated that the changes in ciliary muscle, zonular attachment, ocular rigidity, choroid, and vitreous membrane have a role in the mechanism of the loss of accommodation.[6–8]

Surgical management for the correction of presbyopia can be divided into nonaccommodative treatment,

such as multifocal intraocular lens (IOL) implantation or conductive keratoplasty, and accommodative treatments, such as scleral surgery or accommodating IOLs.[3] Scleral surgical procedures began in 1997 with anterior ciliary sclerotomy (ACS).[9] The ACS procedure used radial incisions in the sclera overlying the ciliary muscle.[9] The aim was to weaken or alter the sclera over the ciliary body to allow for more passive expansion of ciliary body. According to Schachar,[10] increasing the space between the lens equator and ciliary body can place more resting tension on the equatorial zonules, allowing for increased tension to develop during ciliary muscle contraction with resultant restoration of accommodative amplitude.[8] Fukasaku and Marron[11] reported a good initial effect with a mean increase in the accommodative amplitude of 2.2 diopters (D) following ACS. However, gradual regression was observed after the surgery, and only a 0.8-D increase in accommodation was achieved at postoperative 18 months. The authors attributed the regression to the healing response of the sclera.

As opposed to traditional ACS in which a diamond keratotomy knife was used to create 4 to 12 incisions,[3] scleral laser excision or microexcision, using an erbium-doped yttrium aluminum garnet (Er:YAG) laser, was proposed.[12,15–17] Scleral laser microexcisions are based on VisioDymanics theory, a biomechanical model for the aging eye[12] that asserts that presbyopia is not solely the loss of accommodative ability but also the changes in ocular connective tissue that have an impact on ocular biomechanics and function.[13,14] Among the laser scleral procedures, the Laser Anterior Ciliary Excision (LaserACE) (Ace Vision Group, Newark, CA, USA) aims to alter the biomechanical properties of the sclera and reduce the ocular rigidity by creating a series of micropores in sclera in a predetermined diamond matrix over the ciliary muscles, increasing the plasticity and compliance of the scleral tissue during ciliary muscle contraction, thereby improving the efficiency of the accommodative apparatus.[15–17] The preliminary results of 26 patients treated with the LaserACE technique showed the binocular uncorrected near visual acuity (UNVA) significantly improved from +0.20 logMAR to +0.12 logMAR at 24 months after LaserACE.[17] A case series with long-term follow-up showed that the distance-corrected near visual acuity was preserved and stable up to 13 years following LaserACE, although presbyopia progression was still observed.[16] Further to that, laser scleral microporation (Ace Vision Group, Inc., Newark, CA, USA) is performed with the next-generation laser system (VisioLite Gen II, Newark, CA, USA) and shares a similar treatment aim as LaserACE, to improve the compliance of the sclera while under ciliary muscle forces, by decreasing the scleral biomechanical stiffness with laser micropores. Compared with LaserACE, laser sclera microporation delivers pulses with a diode pulsed solid-state system along with a reduced spot size and reduced pulse length, which may provide a favorable view in the postoperative wound-healing profiles.[18]

Postoperative wound healing and remodeling responses are two known factors related to regression after refractive surgery.[19] Likewise, wound contraction and loss of globe expansion were thought to cause regression after ACS.[11] However, postoperative wound-healing profiles in any forms of scleral surgical procedures for presbyopia correction have not been investigated, and published studies to date have focused on the visual and refractive outcomes but not on the postoperative tissue responses.[15–17] As laser scleral microporation is a relatively new treatment option, understanding the time course of postoperative wound-healing responses would help in proposing strategies to mitigate the regression. The modulating effect of concurrent collagen matrix application treatment[15,20] on the postoperative wound healing was also evaluated in the present study.

Methods

Laser Procedure and Optimization of Laser Parameters

Thirty freshly enucleated porcine eyes with postmortem time [8 hours, obtained from a local abattoir (Primary Industries Pte Ltd, Singapore), were used for the optimization of laser parameters. An Er:YAG laser (VisioLite Gen II) was used to create regions of increased pliability in the sclera at four oblique quadrants. The laser frequency was 100 to 300 Hz, laser power was 0.9 to 1.5 W, and spot size was 225 to 265 µm. In each of the four oblique quadrants, the laser created a series of 42 to 49 micropores in a 5-mm × 5-mm matrix over four of five critical zones (zones 2–5) of physiologic significance (Fig. 1)[15–17]: (1) zone 1, 0.0 to 1.3 mm from the limbus, from the limbus to the superior boundary of the ciliary muscle/scleral spur; (2) zone 2, 1.3 to 2.8 mm from the limbus, from the scleral spur to the inferior boundary of the circular ciliary muscle; (3) zone 3, 2.8 to 4.7mm from the limbus, from the inferior boundary of the circular ciliary muscle to the inferior boundary of the radial ciliary muscle; (4) zone 4, 4.7 to 6.6 mm from the limbus, from the inferior boundary of the radial ciliary muscle to the superior boundary of the posterior vitreous zonule zone; and (5) zone 5, 6.6 to 7.3 mm from the limbus, from the superior boundary

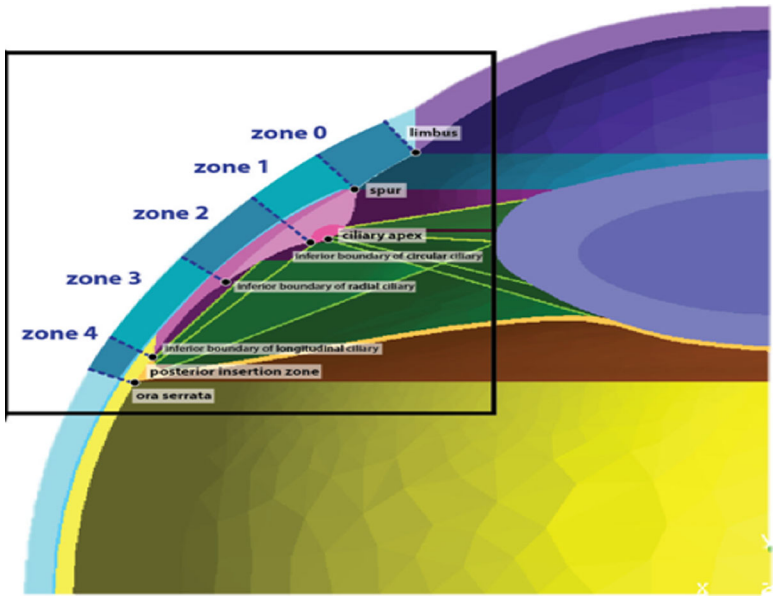

Figure 1. Illustration showing the laser creates a series of micropores in a 5-mm × 5-mm matrix over 4 of 5 critical zones.

of the posterior vitreous zonule zone to the superior boundary of the ora serrata. The laser delivered the same pulses per pore at the same energy levels in each micropore in all zones. Different laser intensities of 8, 12, 15, and 20 pulses/pore were tested in porcine eyes, and the depth of laser micropores on the 17 raster-scan images was measured with the in-built ruler of anterior segment optical coherence tomography (ASOCT; RTVue; Optovue, Inc., Fremont, CA, USA) by an independent observer (NCL).

Study Animals and Experimental Groups

After optimization of laser intensity using porcine eyes, an intensity of 12 pulses/pore was selected for the nonhuman primate study. Six *Macaca fascicularis* monkeys ($n = 12$ eyes), aged 15 to 19 years, were used. The right eye of each animal received the laser treatment as described (L group), and the left eye received the laser treatment with concurrent subconjunctival collagen gel matrix (L + C group). During surgeries and evaluations, the monkeys were tranquilized intramuscularly with ketamine hydrochloride (10 mg/kg) or medetomidine (0.02 mg/kg). Anesthesia was induced with 2% to 3% inhaled isoflurane and maintained with 1% to 2% inhaled isoflurane. For the L + C group, collagen matrix powder (Collamatrix; Chang Gung Biotechnology, Taipei, Taiwan) was mixed with a ratio of 1:4 (v/v) sterile saline solution in a 10-mL syringe. A 0.1-mm peritomy incision was made at the laser areas, and 0.2 mL collagen gel prepared was placed through a cannula into the subconjunctival pocket. An 18-mm scleral contact lens was used to cover the laser areas and hold the collagen gel in place. Topical Tobradex ointment (Alcon, Fort Worth, TX, USA) two times daily for 1 week was used in both eyes after surgery. All surgical procedures were performed by an experienced surgeon (JSM). All animals were treated according to the guidelines of the Association for Research in Vision and Ophthalmology (ARVO) Statement for the Use of Animals in Ophthalmic and Vision Research. The protocol was approved by the Institutional Animal Care and Use Committee (IACUC) of SingHealth, Singapore. The study design of using bilateral surgery in the protocol was approved by the IACUC, as the surgery was not a visually disabling procedure and adhered to the ARVO statement for the use of animals in research.

Clinical Evaluation

All eyes underwent clinical evaluation preoperatively and at 1 week, 2 weeks, 1 month, and monthly thereafter until 9 months postoperatively with slit-lamp biomicroscopy (Nikon FS-3V; Nikon, Tokyo, Japan), tonopen (Tono-Pen AVIA, Reichert, NY, USA) for intraocular pressure (IOP) measurements, and ASOCT for evaluation of the ablation depth. Three IOP measurements and five high-resolution ASOCT cross-sectional scans 5.0 mm away from the limbus were obtained for each eye at each time point. The total scleral thickness, as well as the depth of all the scleral micropores, shown on the ASOCT images, was

measured with the in-built ruler by an independent observer (NCL).

Histology and Immunohistochemistry (IHC) Analysis

At 1, 3, and 9 months postoperatively, two animals (four eyes) were euthanized under anesthesia, and the sclera as well as limbus was excised. The scleral tissue was embedded in an optimal cutting temperature compound at –80°C and cryosectioned at a 5-µm thickness. The sections were then processed for hematoxylin and eosin (H&E) histochemistry using a published protocol[21,22] and visualized under light microscopy (Axioplan 2; Carl Zeiss, Oberkochen, Germany). The area of scleral micropores was measured using the ImageJ software (National Institutes of Health, Bethesda, MD, USA) with the scale bar of light microscopy as a reference scale by a single masked observer (ETWP). For the IHC analysis, the sections were fixed with 4% paraformaldehyde (Sigma, St. Louis, MO, USA) for 15 minutes and blocked for another 15 minutes. The following primary antibodies were then added and incubated for 2 hours at room temperature: mouse monoclonal antibody against cellular fibronectin (MAB-1940; Millipore, Billerica, MA, USA) diluted 1:100, tenascin-C (SC-20932; Santa Cruz Biotechnology, Dallas, TA, USA) diluted 1:200, mouse monoclonal antibody against heat shock protein 47 (HSP47) (ADI-SPA-470; Enzo Life Sciences, Lausen, Switzerland) diluted 1:200, rabbit polyclonal antibody against CD11b (AB-133357; Abcam, Cambridge, UK) diluted 1:100, mouse monoclonal antibody against α–smooth muscle actin (α-SMA) (M0851; Dako, Glostrup, Denmark) diluted 1:100, mouse monoclonal antibody against CD45 (Ab-10558; Abcam) diluted 1:100, mouse monoclonal antibody against CD31 (Ab-199012; Abcam) diluted 1:100, mouse monoclonal antibody against CD90 (LS-B3139; LifeSpan Biosciences, CA, USA) diluted 1:100 and growth-associated protein-43 (GAP43) (NB300-143; Novus Biologicals, Littleton, CO, USA) diluted 1:500, telomerase (MA5-16034, Thermofisher, Waltham, MA, USA) diluted 1:100, and P63 (Sc8431; Santa Cruz Biotechnology, Dallas, TA, USA) diluted 1:50. After washing with 1× phospahte-buffered saline, the sections were incubated with goat anti-mouse Alexa Fluor 488–conjugated secondary antibody or goat anti-rabbit Alexa Fluor 594–conjugated secondary antibody (Invitrogen, Carlsbad, CA, United States) at room temperature for 1 hour. Slides were then mounted with UltraCruz Mounting Medium containing DAPI (Santa Cruz Biotechnology) and were observed and imaged with a Zeiss AxioImager Z1 fluorescence microscope (Carl Zeiss). For the surface or cellular markers (CD11b, CD45, and CD90), the positively staining cells were counted. For the noncellular markers (tenascin-C, α-SMA, fibronectin, HSP47, and GAP43), the staining intensity was evaluated by semiquantifying the mean gray value of the intensity using ImageJ software. All the quantification was performed on three randomly selected sections for each sample at 100× magnification by a single masked observer (ETWP).[23,24]

Statistical Analysis

All data were expressed as mean ± standard deviation (SD). Statistical comparisons between two groups were performed using a Mann-Whitney U test. A repeated-measures analysis of variance was used to compare the values at different time points. Statistical analyses were performed using R (RStudio, Miami, FL, United States) and STATA software (StataCorp, Lakeway, TX, USA). P values less than 0.05 were considered statistically significant.

Results

Optimization of Laser Pulse Intensities

In the optimization experiments using porcine eyes, the mean measured depth of the laser micropores was 32.6% ± 10.5%, 63.5% ± 21.1%, and 83.3% ± 25.8% of the total scleral thickness for the 8, 12, and 15 pulses/pore groups, respectively (Figs. 2A–2C). Scleral perforation was observed when the intensity increased to 20 pulses/pore (Fig. 2D). Hence, 12 pulses/pore was selected for further experiments.

Clinical Evaluation

The preoperative IOP was 13.2 ± 0.8 and 13.0 ± 0.9 mm Hg for the L and L + C groups. The IOP significantly decreased in both groups after the procedure for 7 months (all $P < 0.05$) (Fig. 3). There was no significant difference in the IOP measurements between the L and L + C groups at all time points. On ASOCT evaluation, the margin of the micropores was clearly visible. The mean laser ablation depth for the L and L + C groups was 81.2% ± 5.8% and 76.6% ± 7.2% at 1 month ($P = 0.18$), 77.2% ± 8.2% and 74.8% ± 12.8% at 6 months ($P = 0.25$), and 72.7% ± 11.5% and 71.5% ± 10.5% at 9 months ($P = 0.56$), respectively (Fig. 4). There was a trend of decrease in the ablation depth

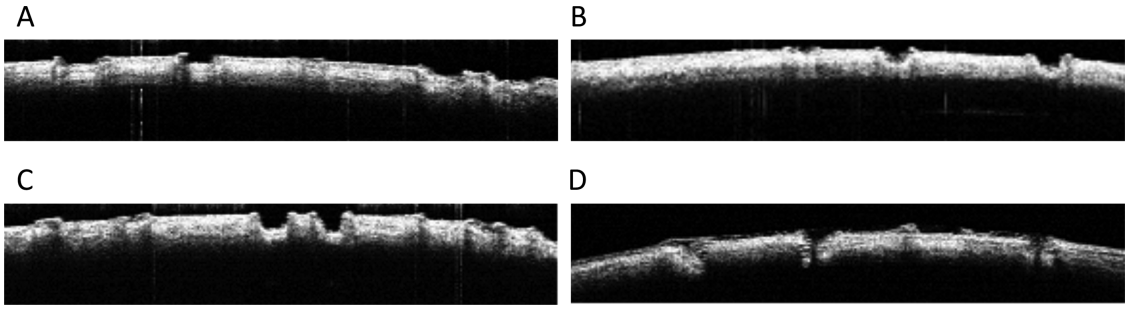

Figure 2. Optimization of laser intensities: 8 (A), 12 (B), 15 (C), and 20 (D) pulses/pore were tested on the porcine eyes, and the laser ablation depth was evaluated by ASOCT. The depth of microspores increased with the increase in the laser intensity (A–C), and scleral perforation was noted when the intensity increased to 20 pulses/pore (D).

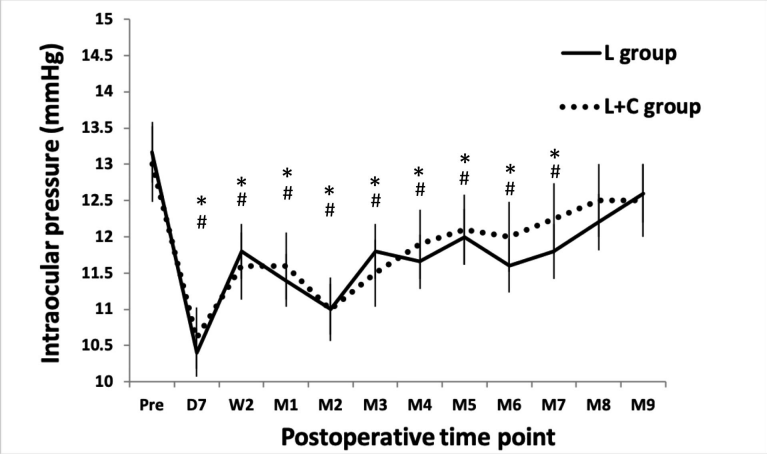

Figure 3. Line graph showing the IOP changes over time following laser scleral microporation for the L and L + C groups. A significant decrease in IOP was observed for 7 months after surgery (* and # indicated $P < 0.05$ for the comparisons of postoperative and preoperative values, for the L and L + C groups) and then gradually increased with time.

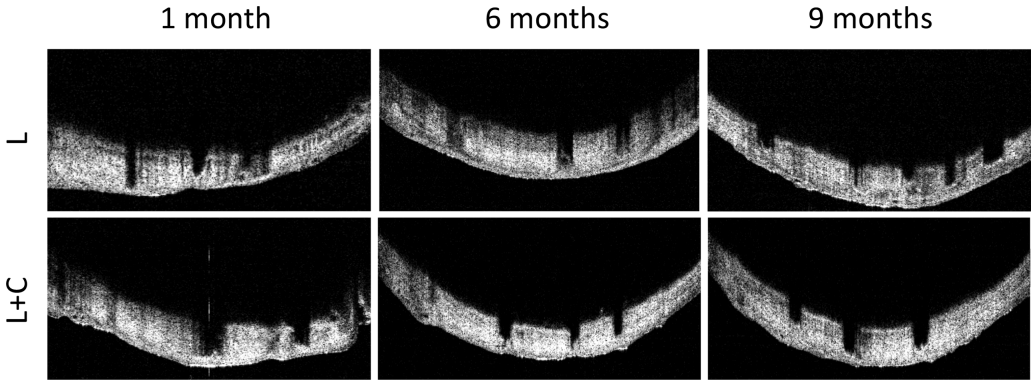

Figure 4. Evaluation of the laser ablation depth by ASOCT. The margin of the scleral micropores was clearly visible. The micropores' depth slightly but not significantly decreased over time, for both L and L + C groups.

over time, but the decrease was not significant ($P = 0.26$ and $P = 0.45$ when comparing postoperative 9 months and 1 month for the L and L + C groups, respectively). On slit-lamp evaluation, no signs of limbal stem cell deficiency, such as recurrent ulceration or irregular corneal surface, were observed in all eyes.

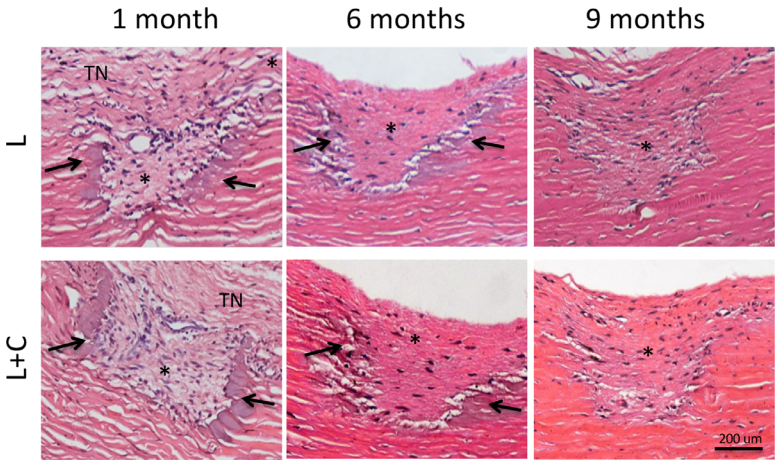

Figure 5. Histologic sections with H&E staining for the L and L + C groups at different time points showed that inflammatory cell infiltration and coagulative necrosis (*arrows*) at 1 month in all eyes, and these responses subsided with time. At 9 months, there were no inflammatory cells or necrosis observed, and the scleral micropores were still patent and filled with fibroblasts. *Asterisk* indicates scleral micropores. TN, Tenon's tissue. Original magnification: 100×. *Scale bar*: 200 µm.

Histologic Analysis

On histologic sections, there was obvious coagulative necrosis, with similar extents in both groups, at the margin of the scleral micropores at postoperative 1 month. The extent of necrosis subsided with time, with a faster rate in the L + C group. Inflammatory infiltrates inside and alongside the margin of micropores were also observed at 1 month but gradually resolved with time. At 6 months, the margin of coagulative necrosis was less distinct. At 9 months, there were no inflammatory cells or necrosis seen, and the scleral micropores were still patent and filled with fibroblasts in all eyes. There was absence of fibrosis or fibrotic encapsulation surrounding the micropores for both groups (Fig. 5). The mean area of micropores, excluding the areas of Tenon's tissue and coagulative necrosis, was 0.09 ± 0.09 and 0.15 ± 0.11 mm^2 at 1 month ($P = 0.45$), 0.12 ± 0.11 and 0.12 ± 0.09 mm^2 at 6 months ($P = 0.38$), and 0.13 ± 0.10 and 0.11 ± 0.09 mm^2 at 9 months ($P = 0.48$) for the L and L + C groups, respectively. There was no significant change in the area measured between different time points for both groups.

Immunohistochemistry Assays

Expression of CD11b and CD45, markers for inflammatory cells and leukocytes, were noticeably detectable surrounding the scleral micropores as well as scleral stroma at postoperative 1 month in both groups (Fig. 6). Quantification of the positively staining cells showed that the L group had significantly more CD11b and CD45 cell infiltration than the L + C group at 1 month ($P = 0.037$ and $P = 0.024$, respectively) (Fig. 7A). The amount of immunostaining significantly decreased from month 1 to month 9 (all P values <0.01 for CD11b and CD45 markers and for both groups) to an indistinct level at 9 months in all eyes.

There was distinct expression of tenascin-C and fibronectin, markers for wound healing, in the scleral tissue surrounding the micropores, particularly alongside the margin of the micropores, throughout the study period. The expression was significantly more apparent in the L than in the L + C group at all time points for tenascin-C staining ($P = 0.018$, $P = 0.042$, and $P = 0.010$, for 1, 6, and 9 months, respectively) and at 1 month for fibronectin staining ($P = 0.001$). There was minimal staining of α-SMA in either scleral micropores or stroma in all eyes at all time points, with no significant difference between two groups. Significantly dense perinuclear staining of HSP47, a collagen-specific stress protein marker, was observed around the micropores in all eyes, with comparable expression in the L and L + C groups. There was also obvious staining of CD90, a marker for fibroblast lineage, at 1 month in all eyes, but the expression significantly decreased at month 9 ($P < 0.01$). For both groups, the staining intensity of tenascin-C, fibronectin, and HSP47 significantly decreased with time ($P = 0.017$ and $P = 0.001$ for the L and L + C groups for tenascin-C; $P = 0.005$ and $P = 0.009$ for the L and L + C groups for fibronectin; $P = 0.002$ and $P = 0.004$ for the L and L + C groups for HSP47, when comparing 9-month intensity with 1-month intensity; Figs. 7B and 8).

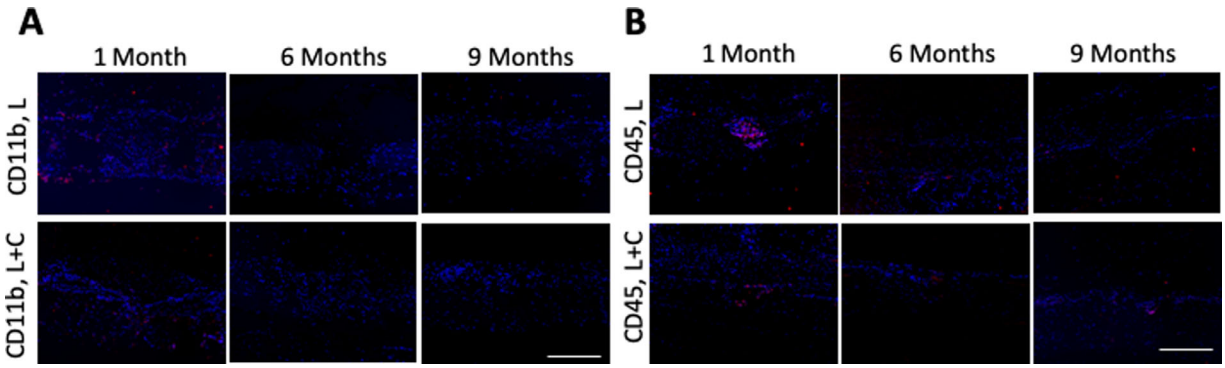

Figure 6. Expression of CD11b and CD45 for the L and L + C groups at different postoperative time points. There was moderate expression of CD11b at 1 month for both groups (A) and obvious staining for CD45 at the micropores at 1 month with less extent in the L + C group (B) in all eyes. The staining amount significantly decreased over time for all markers. Nuclei were counterstained with DAPI (*blue*). Original magnification: 100×. *Scale bar*: 500 µm.

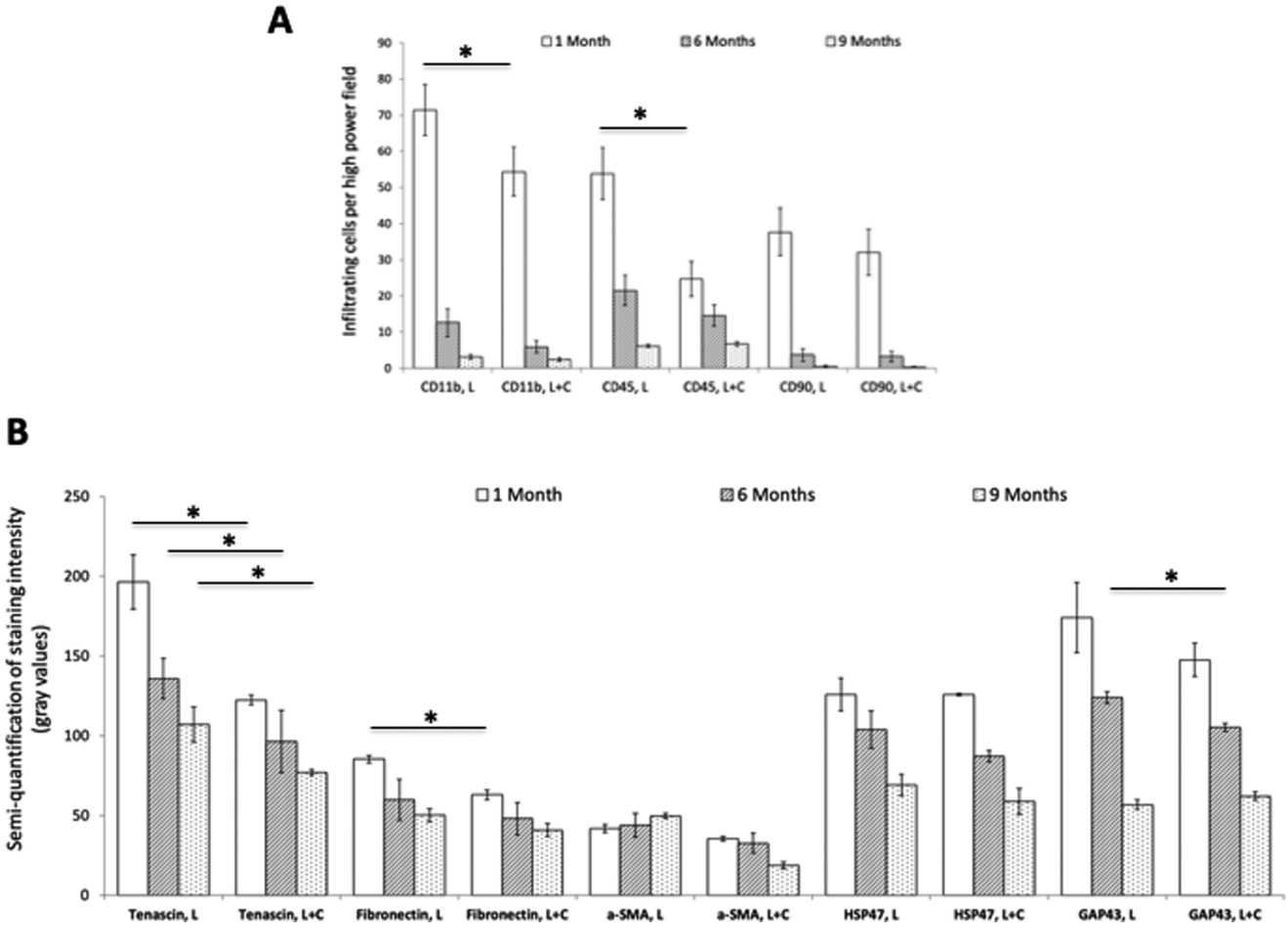

Figure 7. Bar graph showing that the quantification of positively staining cells of the L + C group had significantly less CD11b and CD45-positive cells than L group at 1 month (A; *$P < 0.05$). The evaluation of staining intensity of tenascin-C, fibronectin, α-SMA, HSP47, and GAP43 by semiquantifying the mean gray value of the intensity for the L and L + C groups at different time points (B). *$P < 0.05$.

A marker for damaged axons, GAP43 was significantly upregulated and more obvious at the regions of micropores in all eyes. At 1 month, the expression was comparably high in two groups, and the intensity was significantly lesser in the L + C group at 6 months ($P = 0.002$). At 9 months, the intensity was significantly decreased but still visible in all eyes ($P = 0.011$ and $P = 0.004$ when comparing 9-month intensity with 1-month intensity for the L and L + C groups; Figs. 7 and 8). Expression of CD31, a marker for vascular

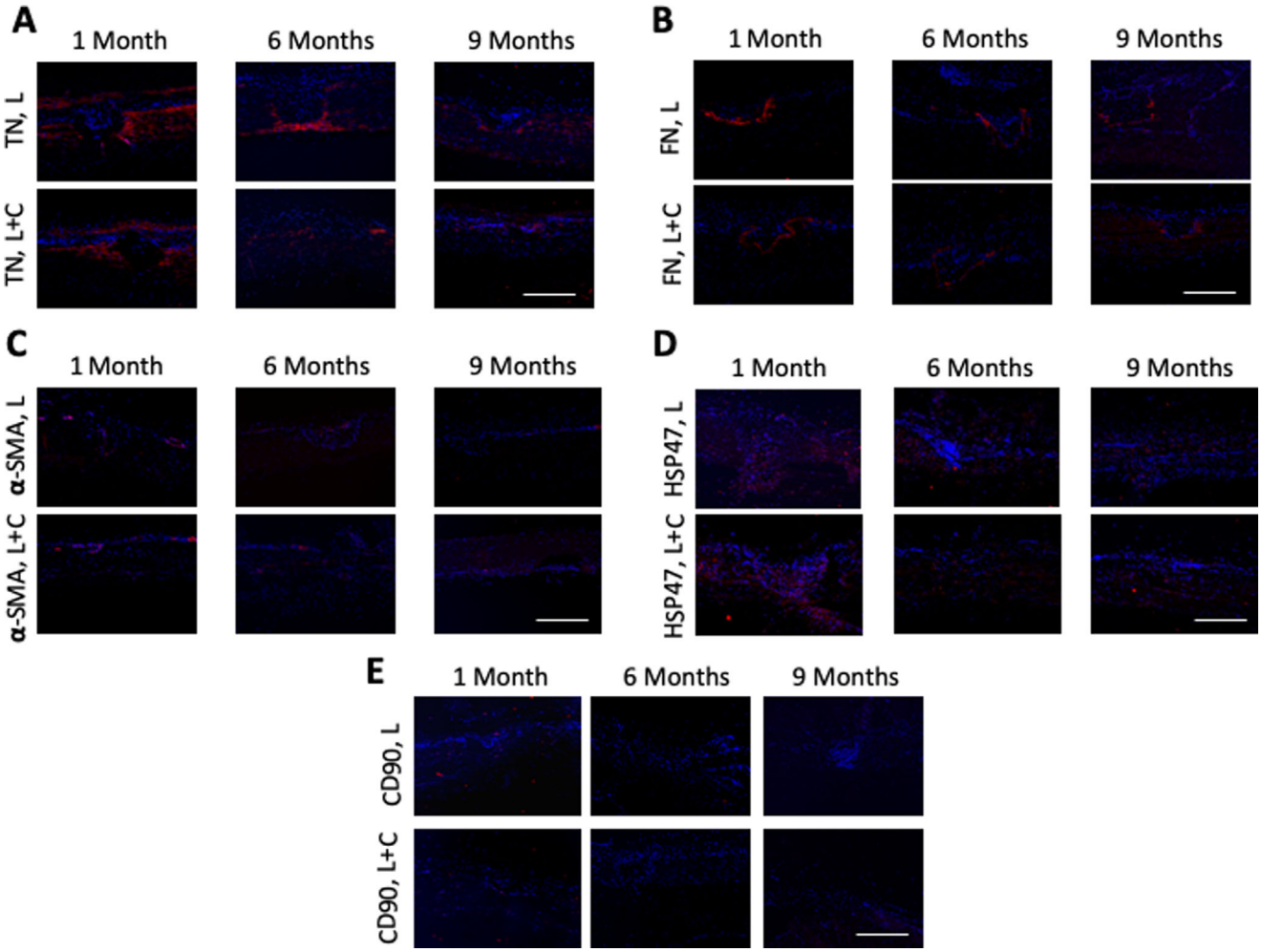

Figure 8. Expression of tenascin-C, fibronectin, α-SMA, HSP47, and CD90 for the L and L + C groups at different time points. The staining was distinct for tenascin-C (TN; A) and fibronectin (FN; B) in all eyes at 1 month, and the extent was lesser in the L + C group than L group. There was minimal staining of α-SMA at all time points in all eyes (C). Significant upregulation of HSP47 was observed in all eyes (D), with comparable expression in L and L + C groups. Moderate expression of CD90 at 1 month in all eyes was seen (E). The staining for all the markers resolved with time. Nuclei were counterstained with DAPI (*blue*). Original magnification: 100×. *Scale bar*: 500 µm.

endothelium, was also observed in the laser-ablated areas with similar intensity at all time points for both groups (Fig. 9).

Limbal stem cell markers, P63 and telomerase, were consistently presented in all eyes. The expression of P63 was observed in the basal layer of the limbus, and telomerase activity was found at the limbus as well as immediate scleral stromal region at all time points (Fig. 10).

Discussion

In the present study, we investigated the tissue responses over time after laser scleral microporation. Postoperative inflammation was self-limited and resolved with time, with minimal response observed 1 month postoperatively. The wound-healing and fibrotic responses were minimal from 6 months onward, and the wound contraction, which may negatively influence the clinical treatment efficacy,[11] was negligible throughout the study period. Concurrent collagen gel matrix application during the procedure could suppress the inflammation and wound-healing responses, which may provide a favorable aspect for longer-lasting treatment efficacy. This is the first study describing the tissue responses following laser scleral procedure for the treatment of presbyopia.

Unlike other surgical procedures for presbyopia, such as corneal laser surgery, multifocal IOLs, or corneal inlay implantation,[25] laser scleral microporation offers several advantages: the visual axes (cornea and lens) are untouched, and theoretically it can

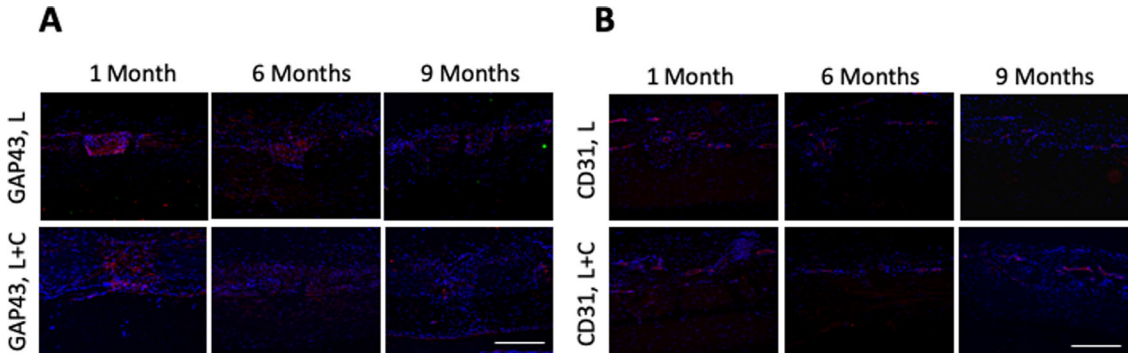

Figure 9. Expression of GAP43 and CD31 for the L and L + C groups at different time points. GAP43 was significantly upregulated with comparable staining intensity for both groups, and it resolved with time (A). Expression of CD31 was also observed around the microspores in all eyes at all time points (B). Nuclei were counterstained with DAPI (*blue*). Original magnification: 100×. *Scale bar*: 500 µm.

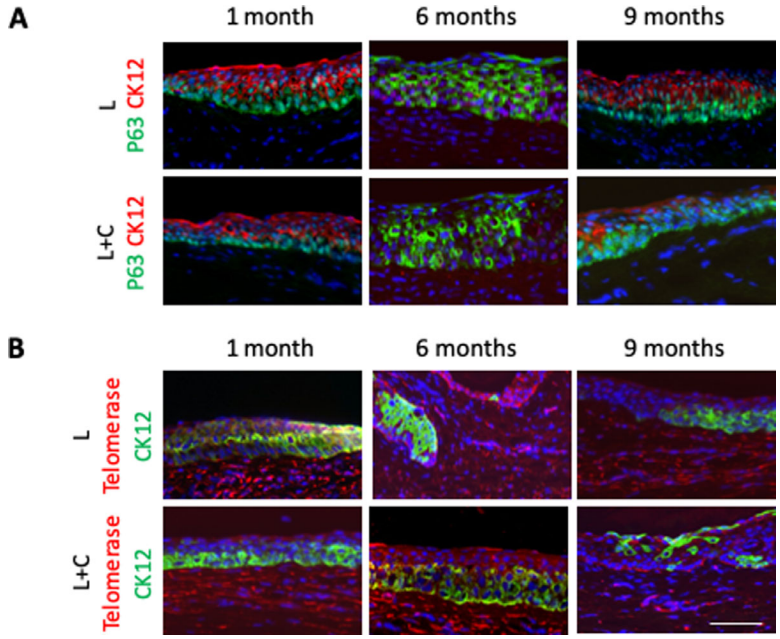

Figure 10. Expression of limbal stem cell markers, P63, and telomerase for the L and L + C groups at different time points. P63-positive cells, stained as *green*, were clearly seen in the limbal areas in both groups. Cytokeratin (CK)–12, a marker for limbal epithelia, were stained as *red* (A). Telomerase activities (*red*) were observed at the limbus and scleral stroma in all eyes. CK-12-positive cells were stained as *green* (B). Nuclei were counterstained with DAPI (*blue*). Original magnification: 200×. *Scale bar*: 500 µm.

be performed after or in combination with other procedures for presbyopia correction.[15,16] A preliminary study on 52 eyes with 24-month follow-up after the LaserACE reported that the binocular UNVA, binocular distance-corrected near visual acuity, and stereoacuity significantly improved postoperatively, and there was no significant change of best-corrected distance visual acuity.[17] However, the underlying wound remodeling that may affect the treatment efficacy and stability has not been elucidated.

The IOP was significantly reduced after surgery for 7 months. The mechanisms of IOP reduction could be localized ciliochoroidal detachment,[26] expansion of the anterior chamber angle, and facilitation of aqueous uveoscleral outflow because an outward expansion of the sclera over the ciliary body–scleral spur area might open the angle and the pore size of the trabecular meshwork or decreased scleral rigidity from the laser micropores.[26,27] The decreased scleral rigidity may also result in an artificially lowered IOP measurement by applanation.[26]

Cadaveric porcine eyes were used to optimize the laser intensity with respect to the depth of the micropores, which will affect the treatment efficacy.[16,17] The micropores were at approximately 63.5% of scleral thickness when the intensity was set at 12 pulses/pore.

As porcine scleral thickness is thicker than human and monkey scleral thickness,[28–30] the intensity of 12 pulses/pore was selected for further monkey study to achieve a targeted depth of 85% to 90%. In the present study, the nonhuman primates used were at presbyopic age, as monkeys' life span is about one-third humans' life span.[31] On the ASOCT evaluation of the monkeys, the micropores were at the depth of 72% to 81% of scleral thickness at 5.0 mm away from the limbus. We found that the depth of micropores decreased over time. Although the measurements were not from longitudinal follow-up but from cross-section evaluation due to the sacrificial time points, the results might suggest that there was some extent of wound remodeling occurring. A study with a longer follow-up period would be considered to investigate the long-term changes. The L + C group had a slower rate of this trend of decrease in the ablation depth than the L group. This is in support of our IHC findings that collagen treatment reduced the tissue responses. There was no significant change in the measured area of the micropores in the histology sections; however, in a histologic assay, the tissue processing for the tissue fixation, sectioning, and staining might interfere the evaluation of the actual depth or width. In the future clinical trial, imaging modalities such as ASOCT as we used in the present study or ultrasound biomicroscopy would be useful to monitor the size of micropores. In addition, the coagulative necrosis shown in the histologic sections might come from the thermal damage during the laser-tissue reaction,[18] but it resolved with time.

When the sclera is stimulated by wounding, the episclera migrates down the scleral wound, supplying vessels, fibroblasts, and inflammatory cells,[32] as shown in our histologic sections. Postoperative wound healing and remodeling have been thought as significant factors influencing the predictability and efficacy of refractive surgery.[19,33] Fukasaku and Marron[11] proposed to implant scleral plugs into the sclerotomy to keep the incisions open to prevent regression. Although it retarded the regression speed, there was still an approximately 1-D regression at 18 months postoperatively. In the histologic analysis in the present study, the depth and width of the micropores did not change significantly with time. These support the notion that controlling or modifying the postoperative wound-healing response may contribute more in the amelioration of regression than mechanically keeping the incisions open. Using a collagen matrix has been known to effectively minimize the postoperative inflammation, fibrogenesis, and angiogenesis[34] in both animal and human studies.[35]

The immunohistochemical analysis showed distinct expression of tenascin-C and fibronectin surrounding the scleral micropores throughout the study period of 9 months, and the collagen treatment suppressed the expression. Tenascin-C has been shown to be involved in the active healing of corneal and scleral wounds, and the expression is indicative of local synthesis.[36] Fibronectin, produced by activated fibroblasts, plays an important role in the wound-healing process. When the wound-healing response is complete, the expression of fibronectin begins to decrease.[37,38] HSP47, a stress response protein, has a profibrogenic role in the wound-healing process and serves as an inducer of collagen production.[39] The expression of HSP47 was abundant and diffuse in the scleral stroma as well as in the micropores at 1 month, with no significant differences between L and L + C groups. α-SMA, a marker for myofibroblast transformation, is linked to wound contraction.[40] The minimal staining of α-SMA in all eyes throughout the study period indicated that the "muscle-like tension" within the scleral micropores acting to pull in the wound margin[40] was not significant after the laser scleral microporation procedure, which is a favorable observation against regression.

Compared with the noticeable wound-healing responses shown in the immunohistochemical studies, the postoperative inflammatory response was mild after postoperative 1 month. CD11b is expressed on the surface of many leukocytes such as monocytes, neutrophils, natural killer cells, granulocytes, and macrophages.[41] CD45 is a leukocyte common antigen, and CD90 is typically a marker for fibroblast lineage during the wound healing.[42] Favorable effects on suppressing the postoperative inflammation were found in the collagen treatment group. Apart from postoperative topical steroid regimen, intraoperative collagen gel application can be considered to reduce surgery-related inflammatory response. Compared with other clinically available drugs such as mitomycin-C or 5-fluorouracil, which are cytotoxic, collagen-based treatment is inherently biocompatible and has been used in a variety of fields, such as trabeculectomy surgery, skin defect, and bone wound, to modulate the wound healing.[20] Collagen is structurally a natural substrate for cellular attachment, proliferation, and differentiation, and functionally, it is chemotactic and modulates cellular responses,[43] such as inflammatory cells and leukocyte responses demonstrated in the present study.

GAP43 is a rapidly transported axonal protein that is highly induced after nerve injury.[44] The distinct expression of GAP43 at the micropores in all eyes indicated the presence of damaged nerves, and it is not unexpected as the intrascleral nerve loops are typically within 3 to 4 mm of the limbus.[32]It was reported that long-term inflammation is associated with the expres-

sion of GAP43.[45] The amount and intensity of staining subsided over time in the present study, and it might be because the inflammation reaction resolved, or there might be some nerve regeneration activity. No obvious scleral vascularization was seen in the H&E sections, while in the immune-staining sections, positive CD31 cells were observed at the micropore areas, with a comparable extent in both groups. However, it could not be differentiated whether the staining was from existing scleral vessels or from the neovascularization due to the laser procedure. P63 protein is normally highly expressed in the limbus and is important in the maintenance of stem cellness as well as the development of stratified epithelia.[46] Telomerase activities, which are present in normal tissue stem cells, were also seen at the limbus.[47] The positive staining of these two markers at limbal areas suggested that the limbal stem cell activity after laser procedure was still maintained. Clinically, no signs of limbal stem cell deficiency, such as corneal wavelike irregularity or recurrent ulceration, were observed in all eyes.

Due to the strict ethical regulation on the use of nonhuman primates, a larger sample size and a sample size with a longer follow-up period or with the inclusion of control group were not allowed. However, nonhuman primates are the most appropriate animal model to study the postoperative tissue response as primates share the highest ocular similarities and genetic homologies with human[48] compared with other animal models such as rabbits or rats. There are also more antibodies available for IHC analysis when using a monkey study than using a porcine model. Furthermore, for further studies investigating the treatment efficacy, a monkey model is the best model as its accommodative apparatus and mechanism are very similar to that of the human, and monkeys' accommodation declines on an essentially identical relative time scale to that of humans.[6]

In conclusion, the postoperative inflammatory reaction following laser scleral microporation was minimal. Scleral wound-healing and fibrotic responses were observed postoperatively but resolved with time. Wound contraction, the tissue response against long-term treatment stability, was not distinct. Concurrent collagen matrix application could provide a favorable role in halting postoperative regression by suppressing the inflammatory and wound-healing responses. Postoperative IOP reduction was also observed. As studies on laser scleral procedures for presbyopia are limited, our results provide better understanding of this new procedure on its time course of postoperative tissue responses. It may be also useful in the development of strategies to improve the long-term stability of this procedure.

Acknowledgments

Supported by the SingHealth Foundation Grant (SHF/FG624S/2014), Singapore.

Disclosure: **Y.-C. Liu**, None; **B. Hall**, None; **N.C. Lwin**, None; **E.P.W. Teo**, None; **G.H.F. Yam**, None; **A. Hipsley**, VisioLite Gen II (P); **J.S. Mehta**, None

References

1. Konstantopoulos A, Liu YC, Teo EP, Lwin NC, Yam GH, Mehta JS. Early wound healing and refractive response of different pocket configurations following presbyopic inlay implantation. *PLoS One*. 2017;12:e0172014.
2. Lindstrom RL, Macrae SM, Pepose JS, Hoopes PC, Sr. Corneal inlays for presbyopia correction. *Curr Opin Ophthalmol*. 2013;24:281–287.
3. Hamill MB, Berdy GJ, Davidson RS, et al. *Refractive Surgery: Section 13, Basic and Clinical Science Course*. 2015–2016 ed. San Francisco, CA: American Academy of Ophthalmology; 2016:153–164.
4. Brown N. The change in shape and internal form of the lens of the eye on accommodation. *Exp Eye Res*. 1973;15:441–459.
5. Koretz JF, Cook CA, Kaufman PL. Aging of the human lens: changes in lens shape upon accommodation and with accommodative loss. *J Opt Soc Am A Opt Image Sci Vis*. 2002;19:144–151.
6. Croft MA, McDonald JP, Katz A, Lin TL, Lutjen-Drecoll E, Kaufman PL. Extralenticular and lenticular aspects of accommodation and presbyopia in human versus monkey eyes. *Invest Ophthalmol Vis Sci*. 2013;54:5035–5048.
7. Croft MA, Nork TM, McDonald JP, Katz A, Lutjen-Drecoll E, Kaufman PL. Accommodative movements of the vitreous membrane, choroid, and sclera in young and presbyopic human and nonhuman primate eyes. *Invest Ophthalmol Vis Sci*. 2013;54:5049–5058.
8. Hamilton DR, Davidorf JM, Maloney RK. Anterior ciliary sclerotomy for treatment of presbyopia: a prospective controlled study. *Ophthalmology*. 2002;109:1970–1976.
9. Azar DT, Koch DD. *Hyperopia and Presbyopia*. New York, NY: Marcel Dekker; 2003:246–288.
10. Schachar RA. Cause and treatment of presbyopia with a method for increasing the amplitude of accommodation. *Ann Ophthalmol*. 1992;24:445–447.

11. Fukasaku H, Marron JA. Anterior ciliary sclerotomy with silicone expansion plug implantation: effect on presbyopia and intraocular pressure. *Int Ophthalmol Clin*. 2001;41:133–141.
12. Garg A, Urzua GA, Dementiev D, Pinelli . *Step by Step Innovations in Presbyopia Management*. New Delhi, India: Jaypee Brothers Medical Publishers; 2006:212–284.
13. Schofield JD, Weightman B. New knowledge of connective tissue ageing. *J Clin Pathol Suppl. (R Coll Pathol)*. 1978;12:174–190.
14. Bailey AJ. Molecular mechanisms of ageing in connective tissues. *Mech Ageing Dev*. 2001;122:735–755.
15. Hipsley A, Hall B, Rocha KM. Scleral surgery for the treatment of presbyopia: where are we today? *Eye Vis (Lond)*. 2018;5:4.
16. Hipsley A, Hall B, Rocha KM. Long-term visual outcomes of laser anterior ciliary excision. *Am J Ophthalmol Case Rep*. 2018;10:38–47.
17. Hipsley A, Ma DH, Sun CC, Jackson MA, Goldberg D, Hall B. Visual outcomes 24 months after LaserACE. *Eye Vis (Lond)*. 2017;4:15.
18. Wang X, Ishizaki NT, Matsumoto K. Healing process of skin after CO2 laser ablation at low irradiance: a comparison of continuous-wave and pulsed mode. *Photomed Laser Surg*. 2005;23:20–26.
19. Liu YC, Rosman M, Mehta JS. Enhancement after small-incision lenticule extraction: incidence, risk factors, and outcomes. *Ophthalmology*. 2017;124:813–821.
20. Chattopadhyay S, Raines RT. Review collagen-based biomaterials for wound healing. *Biopolymers*. 2014;101:821–833.
21. Liu YC, Peng Y, Lwin NC, Venkatraman SS, Wong TT, Mehta JS. A biodegradable, sustained-released, prednisolone acetate microfilm drug delivery system effectively prolongs corneal allograft survival in the rat keratoplasty model. *PLoS One*. 2013;8:e70419.
22. Liu YC, Peng Y, Lwin NC, Wong TT, Venkatraman SS, Mehta JS. Optimization of subconjunctival biodegradable microfilms for sustained drug delivery to the anterior segment in a small animal model. *Invest Ophthalmol Vis Sci*. 54:2607–2615.
23. Liu YC, Ng XW, Teo EPW, et al. A biodegradable, sustained-released, tacrolimus microfilm drug delivery system for the management of allergic conjunctivitis in a mouse model. *Invest Ophthalmol Vis Sci*. 2018;59:675–684.
24. Liu YC, Ang HP, Teo EP, Lwin NC, Yam GH, Mehta JS. Wound healing profiles of hyperopic-small incision lenticule extraction (SMILE). *Sci Rep*. 2016;6:29802.
25. Liu YC, Teo EPW, Ang HP, et al. Biological corneal inlay for presbyopia derived from small incision lenticule extraction (SMILE). *Sci Rep*. 2018;8:1831.
26. Law SK, Syed HM, Caprioli J. Glaucoma care in a patient with previous anterior ciliary sclerotomy and scleral expansion procedure. *Arch Ophthalmol*. 2003;121:1646–1648.
27. Marmer RH. The surgical reversal of presbyopia: a new procedure to restore accommodation. *Int Ophthalmol Clin*. 2001;41:123–132.
28. Olsen TW, Sanderson S, Feng X, Hubbard WC. Porcine sclera: thickness and surface area. *Invest Ophthalmol Vis Sci*. 2002;43:2529–2532.
29. Vurgese S, Panda-Jonas S, Jonas JB. Scleral thickness in human eyes. *PLoS One*. 2012;7:e29692.
30. Girard MJ, Suh JK, Bottlang M, Burgoyne CF, Downs JC. Biomechanical changes in the sclera of monkey eyes exposed to chronic IOP elevations. *Invest Ophthalmol Vis Sci*. 2011;52:5656–5669.
31. Tigges J, Gordon TP, McClure HM, Hall EC, Peters A. Survival rate and life span of rhesus monkeys at the Yerkes regional primate research center. *Am J Primatol*. 1988;15:263–273.
32. Sutphin JE, Dana MR, Florakis GJ, et al. *External Disease and Cornea: Section 8, Basic and Clinical Science Course*. 2015–2016 ed. San Francisco, CA: American Academy of Ophthalmology; 2007:386.
33. Hersh PS, Schein OD, Steinert R. Characteristics influencing outcomes of excimer laser photorefractive keratectomy. Summit photorefractive keratectomy phase III study group. *Ophthalmology*. 1996;103:1962–1969.
34. Ruszczak Z. Effect of collagen matrices on dermal wound healing. *Adv Drug Deliv Rev*. 2003;55:1595–1611.
35. Narayanaswamy A, Perera SA, Htoon HM, et al. Efficacy and safety of collagen matrix implants in phacotrabeculectomy and comparison with mitomycin C augmented phacotrabeculectomy at 1 year. *Clin Exp Ophthalmol*. 2013;41:552–560.
36. Maseruka H, Ridgway A, Tullo A, Bonshek R. Developmental changes in patterns of expression of tenascin-C variants in the human cornea. *Invest Ophthalmol Vis Sci*. 2000;41:4101–4107.
37. Tervo K, Latvala T, Suomalainen VP, Tervo T, Immonen I. Cellular fibronectin and tenascin in experimental perforating scleral wounds with incarceration of the vitreous. *Graefes Arch Clin Exp Ophthalmol*. 1995;233:168–172.
38. Tervo K, van Setten GB, Beuerman RW, Virtanen I, Tarkkanen A, Tervo T. Expression of tenascin and cellular fibronectin in the rabbit cornea after

anterior keratectomy. Immunohistochemical study of wound healing dynamics. *Invest Ophthalmol Vis Sci*. 1991;32:2912–2918.
39. Miyamoto T, Saika S, Yamanaka A, Kawashima Y, Suzuki Y, Ohnishi Y. Wound healing in rabbit corneas after photorefractive keratectomy and laser in situ keratomileusis. *J Cataract Refract Surg*. 2003;29:153–158.
40. Jester JV, Petroll WM, Barry PA, Cavanagh HD. Expression of alpha-smooth muscle (alpha-SM) actin during corneal stromal wound healing. *Invest Ophthalmol Vis Sci*. 1995;36:809–819.
41. Moorthy RS, Davis J, Foster CS, et al. *Intraocular inflammation and Uveitis: Section 9, Basic and Clinical Science Course*. 2015–2016 ed. San Francisco, CA: American Academy of Ophthalmology; 2007:19–26.
42. Pei Y, Sherry DM, McDermott AM. Thy-1 distinguishes human corneal fibroblasts and myofibroblasts from keratocytes. *Exp Eye Res*. 2004;79:705–712.
43. Kallis PJ, Friedman AJ. Collagen powder in wound healing. *J Drugs Dermatol*. 2018;17:403–405.
44. Chaudhary S, Namavari A, Yco L, et al. Neurotrophins and nerve regeneration-associated genes are expressed in the cornea after lamellar flap surgery. *Cornea*. 2012;31:1460–1467.
45. Di Sebastiano P, Fink T, Weihe E, Friess H, Innocenti P, Beger HG, Büchler MW. Immune cell infiltration and growthassociated protein 43 expression correlate with pain in chronic pancreatitis. *Gastroenterology*. 1997;112:1648–1655.
46. O'Sullivan F, Clynes M. Limbal stem cells, a review of their identification and culture for clinical use. *Cytotechnology*. 2007;53:101–106.
47. Shay JW, Wright WE. Telomeres and telomerase in normal and cancer stem cells. *FEBS Lett*. 2010;584:3819–3825.
48. Augusteyn RC, Maceo Heilman B, Ho A, Parel JM. Nonhuman primate ocular biometry. *Invest Ophthalmol Vis Sci*. 2016;57:105–114.